Three-Dimensional Microvascular Fiber-Reinforced Composites

Aaron P. Esser-Kahn, Piyush R. Thakre, Hefei Dong, Jason F. Patrick, Vitalii K. Vlasko-Vlasov, Nancy R. Sottos, Jeffrey S. Moore, and Scott R. White**

Living systems rely on pervasive vascular networks to enable a plurality of biological function in both soft and hard tissue. Extensive vasculature in composite structures, such as osseous tissue in bone and tracheary elements in trees, exemplify natural materials that are lightweight, high-strength, and capable of mass and energy transport. In contrast, synthetic composites possess high strength-to-weight ratios but lack the dynamic functionality of their natural counterparts. The creation of microvascular networks in composites by methods that are fully compatible with current composite manufacturing processes remains an unmet challenge. Fabrication approaches such as laser micromachining,[1–3] soft lithography,[4–7] electrostatic discharge,[8] fugitive inks,[9–11] sugar and polyethylene fibers,[12,13] and hollow glass fibers[14–17] produce microvascular structures, but none of these are suitable for rapid, large-scale production of fiber-reinforced composites with complex vasculatures due to either incompatibility with existing composites manufacturing methods and materials or lack of scalability and vascular complexity of the fabrication approach. Here we show that the introduction of sacrificial fibers into woven preforms enables the seamless fabrication of 3D microvascular composites that are both strong and multifunctional. Underpinning the method is the efficient thermal depolymerization of catalyst-impregnated polylactide (PLA) fibers with simultaneous evaporative removal of the resulting lactide monomer. The hollow channels produced are high-fidelity inverse replicas of the original fiber's diameter and trajectory. The method has yielded microvascular fiber-reinforced composites with channels over one meter in length that can be subsequently filled with a variety of liquids including aqueous solutions, organic solvents, and liquid metals. By circulating fluids with unique physical properties, we demonstrate the ability to create a new generation of biphasic pluripotent composite materials in which the solid phase provides strength and form while the liquid phase provides interchangeable functionality.

Dr. A. P. Esser-Kahn, Prof. J. S. Moore
Chemistry Department
Beckman Institute for Advanced Science and Technology
University of Illinois at Urbana-Champaign
Urbana, IL 61801, USA
E-mail: jsmoore@illinois.edu
Dr. P. R. Thakre
Beckman Institute for Advanced Science and Technology
University of Illinois at Urbana-Champaign
Urbana, IL 61801, USA
H. Dong, Prof. N. R. Sottos, Prof. J. S. Moore
Materials Science and Engineering Department
Beckman Institute for Advanced Science and Technology
University of Illinois at Urbana-Champaign
Urbana, IL 61801, USA
J. F. Patrick
Civil and Environmental Engineering Department
Beckman Institute for Advanced Science and Technology
University of Illinois at Urbana-Champaign
Urbana, IL 61801, USA
V. K. Vlasko-Vlasov
Materials Science Division
Argonne National Laboratory
Argonne, IL 60439, USA
Prof. S. R. White
Aerospace Engineering Department
Beckman Institute for Advanced Science and Technology
University of Illinois at Urbana-Champaign
Urbana, IL 61801, USA
E-mail: swhite@illinois.edu

DOI: 10.1002/adma.201100933

Microvascular composite fabrication begins with the mechanized weaving of sacrificial fibers into 3D woven glass preforms (**Figure 1**a,e). The position, length, diameter, and curvature of fibers are varied to meet the desired design criteria. The interstitial pore space between fibers is infiltrated with a low-viscosity thermosetting resin (e.g., epoxy) and cured at elevated temperature. (Figure 1b,f) After curing, the sample is trimmed to expose the ends of the sacrificial fiber. The fiber is then removed by heating the sample above 200 °C to vaporize the PLA, yielding empty channels and a 3D vascular network throughout the composite (Figure 1c,g). We refer to this process as vaporization of sacrificial components (VaSC). The microvascular composite is then filled with a fluid having the desired physical properties to create a multifunctional material (Figure 1d,h).

The sacrificial fibers used in the VaSC process must satisfy several criteria. First, the fiber must be strong enough to survive the mechanical weaving and vacuum infiltration process. Second, for the creation of complex geometries and large length-to-diameter aspect ratios, the fiber must remain solid during matrix curing (e.g., up to 180 °C) but then be easily removed via depolymerization to monomer vapor at higher temperatures (**Figure 2**a). Finally, the depolymerization and gas production temperature must exist in a narrow range between the highest resin cure temperatures and lowest thermal degradation temperatures (200–240 °C).[18] Here, we report a process using commercially available materials that satisfies all of these criteria.

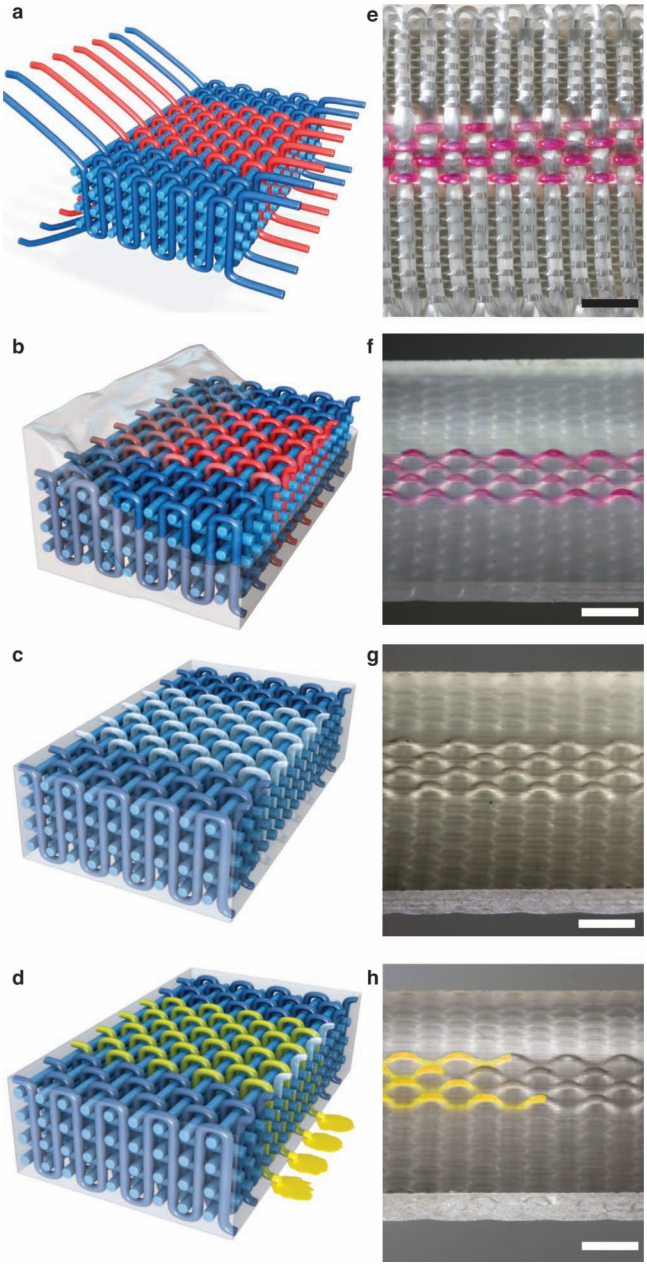

Figure 1. VaSC fabrication procedure. Schematic diagrams of a) straight warp and weft yarns (light blue) with interwoven *Z*-fiber tows (dark blue) and sacrificial fibers (red) to form an orthogonal 3D structure; b) epoxy resin infuses the preform; c) thermal depolymerization and monomer vaporization results in a 3D microvascular network integrated into a structural composite; d) fluid (yellow) fills the microvascular channels. Optical images of e) sacrificial fibers (pink) woven into 3D glass fiber mat; f) resin infiltrated 3D composite; g) empty microvascular network; and h) fluid filling the channels. Scale bars = 5 mm.

PLA is a thermoplastic that spontaneously depolymerizes into gaseous lactide monomers at temperatures above 280 °C.[19] The depolymerization temperature is lowered by the addition of metal catalysts (Figure 2b).[20] We infused fibers with a tin oxalate (SnOx) catalyst, building upon a procedure that allows the incorporation of exogenous chemicals into PLA fibers via a combination of trifluoroethanol (TFE) and water.[21] Exposing fibers to a solution of TFE:H_2O using a ratio of 67:33 (wt%) with 2% SnOx (wt%) for a minimum of 24 h yielded sacrificial fibers suitable for VaSC. The optimization of the fiber treatment procedure will be reported in a subsequent publication.[22] Catalyst-treated fibers converted to gas at a lower temperature and in less time as measured by isothermal gravimetric analysis (iTGA) indicating a lower depolymerization onset temperature (Figure 2c).

Sacrificial fibers were mechanically tested to ensure compatibility with fiber preform fabrication. Sacrificial fibers of diameter 200 and 500 μm were tested to failure using a single fiber tension test. The fiber failure strengths after 24 h treatment were found to be 192 MPa and 351 MPa for 200 μm and 500 μm fibers, respectively. Sacrificial fiber strength far exceeds the threshold stress of 23 MPa applied during automated weaving and both diameters of fiber were successfully woven.

When incorporated into a resin matrix, the sacrificial fiber is removed by heating at 200 °C for several hours. Using a temperature controlled stage and optical microscope, the process of fiber removal was observed. The fiber melts first and then produces gas bubbles that expel liquid out of the channel ends leaving residual material to evaporate, finally resulting in complete clearing of the channel (Figure 2d). Fiber removal typically occurs over the period of 24 h, with 95% of the material removed in less than 6 h. At these temperatures, the initially clear and colorless epoxy matrix is slowly discolored upon exposure to oxygen. Under vacuum (1 Torr) samples display less color change going from colorless to golden-amber. This discoloration occurs primarily at the surface and had no significant impact on mechanical properties of the sample as seen from dynamic mechanical analysis (see Supporting Information S-10).

VaSC can generate a range of channel curvatures and diameters and is suitable for preparing channel interconnects and branched structures. Microchannels ranging in size from 20–500 μm have been created in epoxy matrices following fiber clearing. Empty channels and openings were observed using optical and scanning electron microscopy (Figure 2e). Curvature appears to have minimal effect on the removal of the fiber with both straight and curved channels being cleared completely under standard conditions (see Supporting Information S-3). Interconnections for 3D networks were created using two techniques. In the first case, a cross-junction was formed by overlapping two perpendicular fibers, whereby direct contact was maintained through the application of tension along the fibers. Application of VaSC to this configuration resulted in the formation of interconnected channels at the point of fiber contact, which was confirmed by microscale X-ray computed tomography (μCT) (Figure 2f). For the case of two overlapping 500 μm diameter fibers, an interconnect region of 190 μm across was measured by μCT, matching measurements made by optical microscopy of 210 μm ± 30 μm. In the second case, TFE solvent was used to partially dissolve the PLA and weld the overlapping fibers together at various points of contact. For solvent welded fibers, the average distance across an interconnect region was 318 μm ± 22 μm, as measured by optical microscopy. A multiscale, branched, rootlike vascular network was created by solvent welding a branch of 20 μm fibers to a

ADVANCED MATERIALS
www.advmat.de

www.MaterialsViews.com

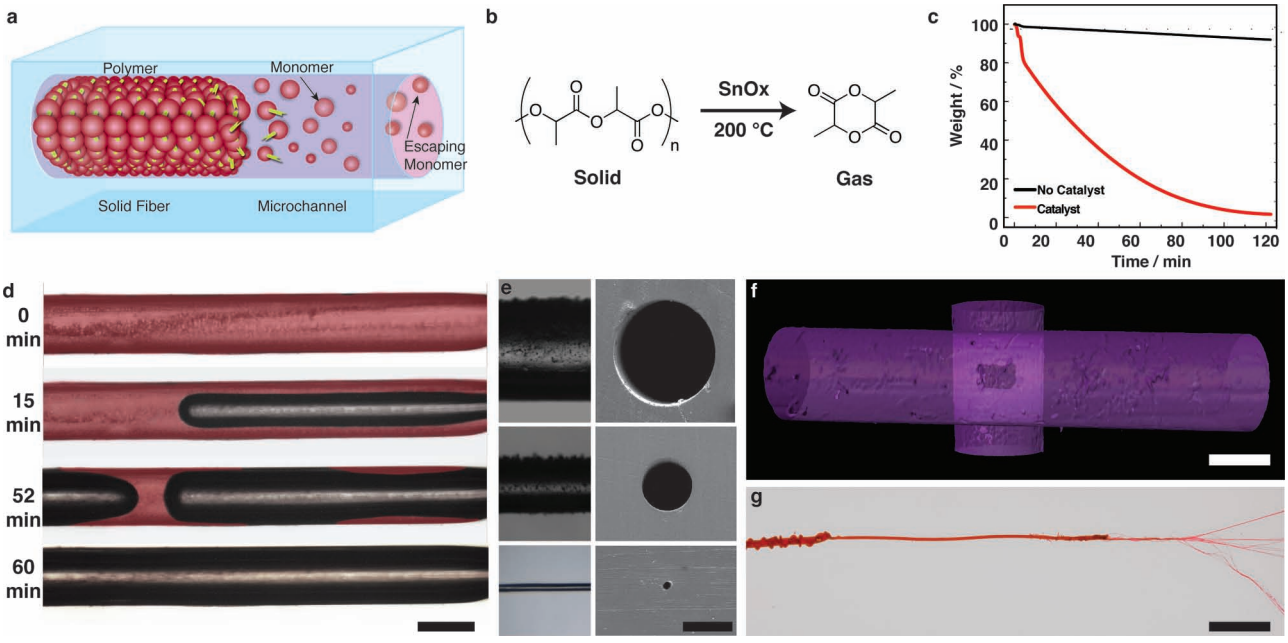

Figure 2. Sacrificial fiber chemistry and microchannel features. a) Schematic mechanism of channel clearing; b) the catalyzed depolymerization reaction of PLA fiber; c) isothermal gravimetric analysis (240 °C) of fibers with (red) and without (black) catalyst; d) optical microscopy images showing the time evolution of fiber clearing (scale bar = 200 μm). Remaining fiber has been color enhanced for visualization. e) Cross sections of channels created from fiber diameters of 500, 200, and 20 μm by the VaSC procedure (scale bar = 250 μm); f) μCT image of channel interconnect formed by two tensioned, overlapping 500 μm fibers (scale bar = 500 μm); g) vascular branching of a 500 μm channel into 20 μm channels via intermediate 200 μm channels filled with dyed solution for visualization (scale bar = 0.5 cm).

500 μm fiber via a 200 μm intermediary fiber. After VaSC, the network was filled with a fluid for imaging (Figure 2g). When combined together, these capabilities allow the construction of a wide variety of network architectures.

Incorporating sacrificial fibers using a computer-controlled 3D weaving process enables microvascular composites with unparalleled precision, ease of fabrication, geometric complexity, and design versatility. Sacrificial and glass fibers were woven into a noncrimp orthogonal pattern[23] using a 3D weaving machine[24] (Figure 1e). These samples were infiltrated with epoxy using vacuum-assisted resin transfer molding (VARTM) and cured (Figure 1f). The sacrificial fiber network inside the composite was cleared using VaSC (Figure 1g). The resulting empty microchannels were filled with liquid (Figure 1h). To demonstrate the versatility of VaSC, a sacrificial fiber was woven throughout all three dimensions of a glass fiber preform and vascularized to reveal a single, continuous channel that spells out the letters UIUC over a total length of 0.5 m (Supporting Information Figure 9).

VaSC is a high-fidelity process. The clearing of channels is robust, resulting in no visible obstructions. We evaluated our 3D woven prototypes for possible concealed imperfections by comparing pressure drop through the channels over a range of flow rates with predictions according to the Hagen–Poiseuille[25] relation. The experimental results (see Supporting Information S-7) exhibited little difference from theory at low flow rates, further supporting the notion of geometric uniformity and virtually complete channel clearing. We additionally confirmed the high fidelity of VaSC by verifying the absence of imperfections in the channels using μCT (Supporting Information Figure 3).

As a demonstration of the pluripotency of microvascular composites, different fluids were infiltrated into the 3D microvascular composite, imbuing multiple physical properties without varying the composite's form factor. We present four different examples of dynamic, multifunctional response: thermal management, electromagnetic signature, electrical conductivity tuning, and chemical reactivity. All of these demonstrations, with the exception of chemical reactivity due to optical transparency restrictions, were carried out using the same vascular composite sample, but substituting the functional fluid in the vascular network in each case.

Thermal management of fiber composites is a highly desirable property for many industrial applications.[26] Nature uses microvascular networks for thermal management by transporting thermal energy to the surface of an organism where heat is more rapidly dissipated. With the introduction of flowing water through the four parallel 500 μm channels in our heated 3D microvascular composite, the surface temperature was reduced by nearly 50% as measured from infrared images (**Figure 3**a), demonstrating potential for increasing the operating temperature of a composite material.

Structures that dynamically change their electromagnetic (EM) signature are sought both for the ability to transmit information about their physical state, as well as the converse, the ability to cloak a surrounding EM field. By filling the channels of a 3D microvascular composite with a ferrofluid,[27] the magnetic field in proximity to the composite was modulated. The magnetic flux of the ferrofluid in the 500 μm channels was imaged using a magneto-optical garnet film[28] and the magnetic signature of the composite, seen as bright spots (≈7 Oe) reveals the underlying capillary architecture (Figure 3c).

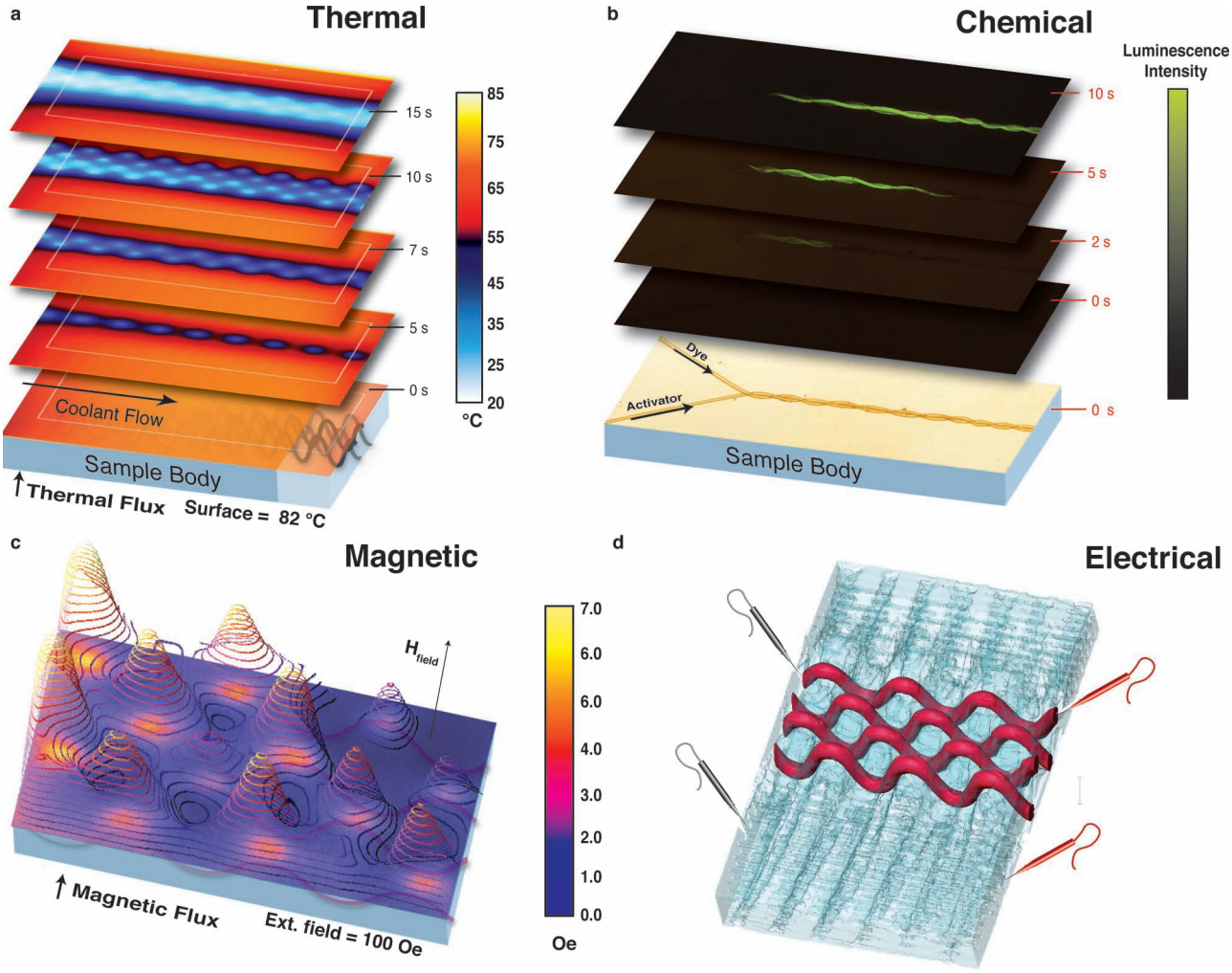

Figure 3. Demonstration of pluripotent microvascular materials. a) Time lapse thermograms recorded from the top surface of a vascularized composite sitting atop a heated substrate (82 °C) and cooled by circulating water (21 °C) through the channels (10 mL min^{-1}). b) Time lapse demonstration of chemical reactivity inside microchannels. A two-part chemiluminescent solution flowed through two connected channels resulting in a luminescent reaction (center, green) inside the material. c) Magneto-optical microscopy image showing out-of-plane H-magnetic field of the 3D composite after being filled with a ferrofluid. d) μCT image of composite with glass fibers (blue) and channels filled with electrically conductive gallium–indium alloy (red). Probe schematics indicate the location of conductivity measurements.

Dynamic tuning of electrical conductivity of composites is a desirable property as a means to transmit information and energy.[29–32] A conductive liquid metal, eutectic gallium–indium (GaIn: 75% Ga, 25% In, wt%), was infiltrated and solidified inside the channels and the microvascular network was imaged using μCT, revealing symmetric placement of electrically conductive channels (Figure 3d). The electrical conductivity along the GaIn channels was measured (4×10^3 S cm^{-1}) to be about seven orders of magnitude higher than the surrounding glass/epoxy composite (10^{-4} S cm^{-1}), demonstrating selectively conductive regions within the same composite (see Supporting Information S-16).

Finally, microvascular networks capable of chemical reactivity are relevant for a range of applications in microfluidics and self-healing systems. As a simple demonstration of a network's ability to perform a chemical reaction, a two-channel mixing network was created. A channel containing a chemiluminescent[32–35] solution was mixed via fiber interconnects with one containing activator. Mixing led to the spontaneous production of light in the channels indicating that a reaction had taken place (Figure 3b).

The creation of pluripotent 3D microvascular fiber reinforced composites enables material systems with unprecedented applications. The VaSC method uses commercially available materials and can be seamlessly integrated with conventional fiber-reinforced composite manufacturing methods. Composites can be designed to contain a spectrum of microvascular network types and sizes from simple, straight conduits to complex computer-controlled 3D woven architectures. VaSC is an enabling platform technology for a wide array of future applications beyond fiber-reinforced structural composites ranging from tissue patterning to gas exchange. Sacrificial fibers provide a tool to reliably create biomimetic material systems capable of reproducing and extending many of the transport functions performed by microvascular systems in nature.

Supporting Information

Supporting Information is available from the Wiley Online Library or from the author.

Acknowledgements

H.D. and J.F.P. contributed equally to this work. This work was supported by the AFOSR through grants FA9550-05-1-0346, FA9550-09-0686, and FA9550-10-1-0255. We also acknowledge the support of the OFA/Department of Homeland Security (project #2008–ST–061-ED002). The authors acknowledge Dr. M. Mohamed and Dr. D. Mungalov of 3TEX Inc. for weaving the 3D fiber preforms containing sacrificial fibers. The authors thank M. Cale and K. Feng for general assistance. The authors thank Beckman ITG as well as Dorothy Loudermilk for assistance in figure creation.

Received: March 11, 2011
Revised: May 20, 2011
Published online: July 15, 2011

[1] D. Lim, Y. Kamotani, B. Cho, J. Mazumder, S. Takayama, *Lab Chip* **2003**, *3*, 318.
[2] K. Lee, R. Kim, D. Yang, S. Park, *Prog. Polym. Sci.* **2008**, *33*, 631.
[3] R. A. Borisov, G. N. Dorojkina, N. I. Koroteev, V. M. Kozenkov, S. A. Magnitskii, D. V. Malakhov, A. V. Tarasishin, A. M. Zheltikov, *Appl. Phys. B: Lasers Opt.* **1998**, *67*, 765.
[4] H. Wu, T. W. Odom, D. T. Chiu, G. M. Whitesides, *J. Am. Chem. Soc.* **2003**, *125*, 554.
[5] B. Jo, L. Van Lerberghe, K. Motsegood, D. Beebe, *JMEMS.* **2000**, *9*, 76.
[6] J. T. Borenstein, E. J. Weinberg, B. K. Orrick, C. Sundback, M. R. Kaazempur-Mofrad, J. P. Vacanti, *Tissue Eng.* **2007**, *13*, 1837.
[7] M. Shin, K. Matsuda, O. Ishii, H. Terai, M. Kaazempur-Mofrad, J. Borenstein, M. Detmar, J. P. Vacanti, *Biomed. Microdevices* **2004**, *6*, 269.
[8] J. Huang, J. Kim, N. Agrawal, A. P. Sudarsan, J. E. Maxim, A. Jayaraman, V. M. Ugaz, *Adv. Mater.* **2009**, *21*, 3567.
[9] D. Therriault, S. R. White, J. A. Lewis, *Nat. Mater.* **2003**, *2*, 265.
[10] C. J. Hansen, W. Wu, K. S. Toohey, N. R. Sottos, S. R. White, J. A. Lewis, *Adv. Mater.* **2009**, *21*, 4143.
[11] K. S. Toohey, N. R. Sottos, J. A. Lewis, J. S. Moore, S. R. White, *Nat. Mater.* **2007**, *6*, 581.
[12] L. M. Bellan, S. P. Singh, P. W. Henderson, J. Porri, H. G. Craighead, J. A. Spector, *Soft Matter* **2009**, *5*, 1354.
[13] L. M. Bellan, E. A. Strychalski, H. G. Craighead, *J. Vac. Sci. Technol. B* **2008**, *26*, 1728.
[14] R. S. Trask, I. P. Bond, *Smart Mater. Struct.* **2006**, *15*, 704.
[15] R. S. Trask, G. Williams, I. P. Bond, *J. R. Soc. Interface* **2007**, *4*, 363.
[16] G. Williams, R. S. Trask, I. P. Bond, *Composites, Part A* **2007**, *38*, 1525.
[17] C. Y. Huang, R. S. Trask, I. P. Bond, *J. R. Soc. Interface* **2010**, *7*, 1229.
[18] L. Lee, *J. Polym. Sci., Part A: Polym. Chem.* **1965**, *3*, 859.
[19] Y. Aoyagi, K. Yamashita, Y. Doi, *Polym. Degrad. Stab.* **2002**, *76*, 53.
[20] Y. Fan, H. Nishida, T. Mori, Y. Shirai, T. Endo, *Polymer* **2004**, *45*, 1197.
[21] R. A. Quirk, M. C. Davies, S. J. B. Tendler, K. M. Shakesheff, *Macromolecules* **2000**, *33*, 258.
[22] H. Dong, A. P. Esser-Kahn, P. R. Thakre, J. F. Patrick, N. R. Sottos, S. R. White, J. S. Moore, unpublished.
[23] A. E. Bogdanovich, M. H. Mohamed, *SAMPE J.* **2009**, *45*, 8.
[24] A. E. Bogdanovich, P. Bradford, D. Mungalov, S. Fang, M. Zhang, R. H. Baughman, S. Hudson, *SAMPE J.* **2007**, *43*, 6.
[25] B. R. Munson, D. F. Young, T. H. Okiishi, *Fundamentals of Fluid Mechanics*, John Wiley & Sons, New York **2002**.
[26] B. D. Kozola, L. A. Shipton, V. K. Natrajan, K. T. Christensen, S. R. White, *J. Intell. Mat. Syst. Struct.* **2010**, *21*, 1147.
[27] N. Pamme, *Lab Chip* **2006**, *6-1*, 24.
[28] V. K. Vlasko-Vlasov, U. Welp, G. W. Crabtree, V. I. Nikitenko, *NATO Adv. Studies Instit., Series E: Appl. Science*, *356*, Kluwer, Dordrecht **1999**, pp. 205.
[29] J. So, J. Thelen, A. Qusba, G. J. Hayes, G. Lazzi, M. D. Dickey, *Adv. Funct. Mater.* **2009**, *19*, 3632.
[30] S. Cheng, Z. Wu, *Lab Chip* **2010**, *10*, 3227.
[31] M. Kubo, X. Li, C. Kim, M. Hashimoto, B. J. Wiley, D. Ham, G. M. Whitesides, *Adv. Mater.* **2010**, *22*, 2749.
[32] M. D. Dickey, R. C. Chiechi, R. J. Larsen, E. A. Weiss, D. A. Weitz, G. M. Whitesides, *Adv. Funct. Mater.* **2008**, *18*, 1097.
[33] H. Shen, Q. Fang, Z.-L. Fang, *Lab Chip* **2006**, *6*, 1387.
[34] M. Hashimoto, K. Tsukagoshi, R. Nakajima, K. Kondo, A. Arai, *J. Chromatogr. A* **2000**, *867*, 271.
[35] E. Wilson, *Chem. Eng. News* **2009**, *77*, 65.